ELSEVIER

Original Articles

Quantitative Proton Magnetic Resonance Spectroscopy of Focal Brain Lesions

Bernd Wilken, MD*, Peter Dechent, Dipl Biol[§], Jochen Herms, MD[†], Caroline Maxton, MD*, Evangelos Markakis, MD[‡], Folker Hanefeld, MD*, and Jens Frahm, PhD[§]

The diagnostic value of single-voxel proton magnetic resonance spectroscopy (2 T, stimulated echo acquisition mode, TR = 6,000 ms, TE = 20 ms, 4-5 mL volumes-of-interest) was assessed for a differentiation of focal brain lesions of unknown etiology in 17 patients 1-14 years of age. Absolute metabolite concentrations were compared with age-matched control subjects and an individual control region. Most of the brain tumors were characterized by strongly reduced total *N*-acetylaspartyl compounds and marked increases of *myo*-inositol and choline-containing compounds, consistent with a lack of neuroaxonal tissue and a proliferation of glial cells. Lactate was elevated in only four patients. When using this pattern for a metabolic discrimination of brain tumors from other focal lesions, proton spectroscopy correctly identified 14 of 17 abnormalities, as confirmed by histologic examination after neurosurgical intervention. One false-positive tumor diagnosis was a severe reactive gliosis mimicking a typical tumor spectrum. Two inconclusive cases comprised an astrocytoma with moderately elevated *myo*-inositol but reduced choline-containing compounds and a patient with an abscess leading to a marked reduction of all metabolites but strong contributions from mobile lipids. In summary, quantitative proton spectroscopy has considerable clinical value for preoperative characterization of focal brain lesions.

Wilken B, Dechent P, Herms J, Maxton C, Markakis E, Hanefeld F, Frahm J. Quantitative proton magnetic resonance spectroscopy of focal brain lesions. Pediatr Neurol 2000;23:22-31.

Introduction

Tumors of the central nervous system are the most common form of childhood solid neoplasms and the leading cause of death from cancer in children younger than 15 years of age [1]. Consistent etiologic factors are not known, and neurobiologic alterations are not understood. Because the clinical presentation of these tumors varies largely depending on type, localization, and growth rate, the differential diagnosis of malignant brain tumors and focal lesions of other origin often poses a problem when based on clinical and neuroradiologic findings alone.

Localized proton magnetic resonance spectroscopy (MRS) provides noninvasive insights into the neurochemistry of normal and pathologic states of the central nervous system. It has technically matured during the past decade and been successfully applied to a large range of cerebral abnormalities in children and adults [2,3]. Although a specific histologic classification or grading of tumors by proton MRS faces complications from a variety of sources [4,5], numerous studies reported consistent differences between neoplastic and normal brain tissue since early descriptions [6]. For recent studies of brain tumors in children see Girard et al. [7] and Norfray et al. [8].

The purpose of this study was to confirm the utility of quantitative single-voxel proton MRS in the differential diagnosis of brain tumors and other focal abnormalities. In particular, we studied 17 children with suspect magnetic resonance imaging (MRI) findings and exploited the characteristic alterations of brain metabolites that are associated with the occurrence of a primary brain tumor (i.e., reduced content or even lack of neuroaxonal tissue and proliferation of glial cells). The prospective value of proton MRS was determined by a comparison with results

From the *Abteilung Kinderheilkunde; Schwerpunkt Neuropädiatrie; [†]Institut für Neuropathologie; and [‡]Klinik für Neurochirurgie of the Georg-August Universität; Göttingen, Germany; and [§]Biomedizinische NMR Forschungs GmbH am Max-Planck-Institut für biophysikalische Chemie, Göttingen, Germany.

Communications should be addressed to:
Dr. Frahm; Biomedizinische NMR Forschungs GmbH am Max-Planck-Institut für biophysikalische Chemie;
D-37070 Göttingen, Germany.
Received November 29, 1999; accepted February 2, 2000.

PII S0887-8994(00)00141-7 • 0887-8994/00/$20.00

Table 1. Summary of patient data

Pt. No./Sex/Age (yr)	Neurologic Symptoms	Location of Lesion	Differential Diagnosis
1/M/3	Epilepsy	Right temporal	Rasmussen encephalitis
2/F/2	Head tilt, ataxia	Left cerebellum	Vascular lesion, tumor
3/M/13	Left spastic hemiparesis, hemiballism	Right thalamus	Inflammation
4/M/12	Double vision, strabismus	Left frontotemporal	Inflammation
5/F/1	Epilepsy after tumor removal/chemotherapy	Left parieto-occipital	Recurrent tumor
6/F/7	Rotatory nystagmus, head tilt, ataxia	Left cerebellum	Gliosis, neurofibromatosis
7/F/6	Headache, vomiting	Midbrain	Heterotopia, tumor
8/F/9	Epilepsy	Left parieto-occipital	Infarction
9/F/2	Dizziness	Right cerebellum	Ischemic lesion, tumor, hamartoma
10/F/9	Headache	Left parieto-occipital	Tumor, metastasis
11/M/3	Behavioral abnormality	Right cerebellar pedunculus	Heterotopia
12/F/9	Epilepsy	Left parieto-occipital	Inflammation, tumor
13/M/12	Paresthesia	Right pons	Inflammation, tumor
14/M/9	Retrobulbar pain	Left frontal	Tumor, gliosis
15/M/14	Behavioral abnormality	Right frontal	Tumor, gliosis
16/F/2	Epilepsy	Left temporal	Heterotopia, tumor
17/M/11	Headache	Right thalamus	Tumor, abscess

Abbreviations:
F = Female
M = Male
Pt. No. = Patient number

from histopathologic examinations after neurosurgical intervention.

Material and Methods

Seventeen patients (mean age = 7.3 years, range = 1-14, nine female, eight male) with suspect focal cerebral lesions and an uncertain diagnosis underwent MRS as part of the diagnostic evaluation. Subsequent neurosurgical intervention ranging from stereotactic biopsy to tumor removal was performed in all children and yielded a histopathologically confirmed diagnosis in all cases. Before each proton MRS examination, informed written consent was obtained from the parents. Proton MRS studies of children were approved by the institutional review board.

The spectrum of clinical symptoms was widespread and ranged from signs of raised intracranial pressure, pareses, movement disorders, such as ataxia or dystonia, and seizures to behavioral problems. None were specific in these children. The differential diagnosis included tumor, gliosis, inflammation, demyelination, vascular malformations, and cortical dysplasias. A summary of patient data is presented in Table 1.

All MR studies were performed at 2.0 T (Magnetom Vision, Siemens, Erlangen, Germany) using either the standard imaging head coil or, for children less than 20 kg bodyweight, the extremity coil. Children younger than 6 years were sedated with chloral hydrate and monitored by pulse oximetry.

Fully relaxed short-echo time proton magnetic resonance (MR) spectra were acquired using a single-voxel stimulated echo acquisition mode localization sequence, as described previously [9,10]. The parameters were TR = 6,000 ms, TE = 20 ms, and TM = 10 ms, with 64 accumulations leading to measuring times of 6.5 minute per spectrum. Volumes-of-interest (VOI) were selected from three sets of orthogonal T_1-weighted images and transverse T_2-weighted images. Typically, MRS included at least two acquisitions, with a 4-5 mL VOI placed inside the focal lesion and in a control region (i.e., preferably a homologue area of the contralateral hemisphere). The spectral evaluation was accomplished with use of LCModel (S. Provencher, Göttingen, Germany), a user-independent fitting routine based on a library of calibrated model spectra of individual metabolites with known absolute concentrations [11]. Concentrations are expressed in mmol per liter VOI, without corrections for cerebrospinal fluid contributions and residual T_2 relaxation effects.

Major detectable brain metabolites include the neuronal markers [12] *N*-acetylaspartate and *N*-acetylaspartylglutamate (tNAA), creatine and phosphocreatine (tCr), choline-containing compounds (Cho), the glial marker [13] *myo*-inositol (Ins), and lactate (Lac). Previous investigations of regional age dependencies of cerebral metabolites in human brain [14] provided age-matched controls for the evaluation of abnormal metabolite concentrations. If suitable data for a particular brain region were not available, the lesion was compared with an individual control region. It should be emphasized that all metabolic assessments were exclusively based on quantitative spectroscopic data obtained by an automated user-independent analysis. The qualitative presentation of manually processed proton MR spectra in this article only serves for easy visual inspection.

Results

The spectroscopic results for all patients are summarized in Table 2, in which metabolite alterations are given as the percentage of deviation from control subjects. Most of the intracranial tumors were characterized by low neuroaxonal and high glial tissue components relative to normal brain. Accordingly, their proton MR spectra comprise low tNAA levels and elevated Ins or Cho concentrations. Lac was detected in only a few patients with brain tumors. In contrast, gliosis mostly resulted in elevated Ins or Cho but only mild or no reduction of tNAA and no Lac. On the basis of the quantitative analysis of the observed metabolite pattern in any individual patient, MRS led to a decision of whether the lesion was consistent with a tumor (Table 2). Typical findings for brain tumors are demonstrated in Figures 1-3, depicting MRI and lesion and control MR spectra of a high-grade anaplastic glioma, a primitive neuroectodermal tumor, and a low-grade astrocytoma, respectively.

Complementing the tabulated summary, we considered

Table 2. Proton MR spectroscopy and histopathologic features of focal brain lesions

Pt. No.	tNAA*	tCr*	Cho*	Ins*	Lac†	Tumor	Histologic Findings‡	Merit
1	−56	−14	−11	+103	−	Yes	Astrocytoma II	Correct
2	−56	−34	+79	+49	−	Yes	Astrocytoma II	Correct
3	−66	+10	+89	+249	−	Yes	Anaplastic glioma III	Correct
4	−47	+3	+100	+51	+	Yes	Astrocytoma I	Correct
5	−74	−12	+144	+280	++	Yes	Primitive neuroectodermal tumor	Correct
6	−59	−36	+48	+136	−	Yes	Astrocytoma I	Correct
7	−40	−22	+150	+14	+	Yes	Astrocytoma II	Correct
8§	−56	+7	+46	+339	−	Yes	Astrocytoma I	Correct
9	−66	−23	+42	+111	+	Yes	Astrocytoma I	Correct
10	−73	−60	+108	+20	Lip	Yes	Ektomesenchymoma	Correct
11§	−64	−11	+36	+51	−	Yes	Astrocytoma I	Correct
12	−80	+35	+6	+227	−	Yes	Gliosis	Wrong
13	−81	−7	−6	+24	−	No	Multiple sclerosis	Correct
14§	−10	+8	+42	+69	−	No	Gliosis	Correct
15§	−17	+3	+38	+60	−	No	Gliosis	Correct
16§	−68	+2	−50	+42	−	Unclear	Astrocytoma II	No value
17	−71	−68	−39	−	Lip	Unclear	Abscess	No value

* Values represent percentage of deviation from age-matched controls [14].
† Lactate values were classified as normal (−), mildly elevated (+), and strongly elevated (++).
‡ Grading according to the World Health Organization.
§ Percentage of deviation from an individual control region.

Abbreviations:
Cho = Choline-containing compounds
Ins = *myo*-inositol
Lac = Lactate
Lip = Strongly elevated resonances from mobile fatty acids
Pt. No. = Patient number
tCr = Creatine and phosphocreatine
tNAA = *N*-acetylaspartate and *N*-acetylaspartylglutamate

it mandatory to present selected cases in more detail. The cases of the three patients discussed below underline the rationale for using patterns of absolute metabolite concentrations to aid in the differential diagnosis of focal brain lesions and further illustrate the role of MRS in clinical decision-making and patient management.

Case Reports

Patient 9. This 2-year-old female had a normal neurologic development. After a head injury caused by falling down three steps of a staircase, she was continuously sleepy. The neurologic examination was normal. Cranial computed tomography revealed a hyperdense area in the right cerebellar hemisphere but no signs of hemorrhage. This lesion was subsequently confirmed by MRI (Fig 3A). The differential diagnosis included an ischemic lesion, a low-grade tumor, or hamartoma.

The proton MR spectra in Figures 3B and 3C revealed increased Cho (2.7 mM compared with 1.2 mM on the contralateral side and 2.0 ± 0.1 mM in a group of 2-5-year-old control children) and a most pronounced elevation of the glial marker Ins (12.9 mM vs 5.5 mM on the contralateral side and 6.2 ± 0.4 mM in the control children). tCr levels in the lesion and on the contralateral side were 6.2 mM and 6.4 mM, respectively, slightly below the 8.6 ± 1.2 mM found in the control children. A clear spectral representation of the neuroaxonal marker tNAA was no longer detected in the lesion. The tNAA concentration on the contralateral side was 6.5 mM (7.0 ± 0.5 in control children). Moreover, the lesion was characterized by mildly elevated Lac (2.8 mM, with contralateral and normal values less than 1 mM). The proton MRS pattern of very low tNAA and high Ins and Cho clearly suggested a tumor.

Neurosurgical intervention led to the complete removal of the tumor. The histopathologic diagnosis was a low-grade astrocytoma. After surgery, the child had a normal developmental and neurologic status.

Patient 14. This 9-year-old male underwent MRI after mild head trauma and complaints about retrobulbar pressure. MRI exhibited signal abnormalities in a left frontal area (Fig 4A). The neurologic examination and all neurophysiologic investigations, such as electroencephalography and evoked potentials, were normal. MRS was performed to further elucidate the nature of the lesion.

The spectra in Figures 4B and C represent mixed contributions from the gray and white matter. They reveal only mildly reduced to normal concentrations of tNAA (6.2 mM vs 6.9 mM on the contralateral side and 8.4-9.6 mM in "pure" frontal gray and white matter of the control children) and tCr (5.2 mM vs 4.8 mM on the contralateral side and 5.7-6.4 mM in the control children). In contrast, the concentration of the glial marker Ins was 5.9 mM in the lesion, well above the 3.5 mM on the contralateral side or the range of 3.8-4.3 mM in the frontal gray and white matter of the control children. Also the Cho concentration of 1.70 mM was much higher than the 1.25 mM in the contralateral homologue area (1.4-1.8 mM in gray and white matter of the control children).

Together with the absence of elevated Lac, this pattern of metabolite alterations may be understood as a mild loss of neuroaxonal tissue (tNAA) in combination with a proliferation of astrocytes (Ins and Cho). It is therefore consistent with gliosis. The neurosurgical exploration and histopathologic examination confirmed the diagnosis of a reactive gliosis.

Patient 17. Two months before MRS, this 11-year-old male with congenital heart disease (double outlet, right ventricle) suffered from headaches on the left side. The patient had no fever because of antibiotic treatment for tonsillitis. The neurologic examination was normal, but

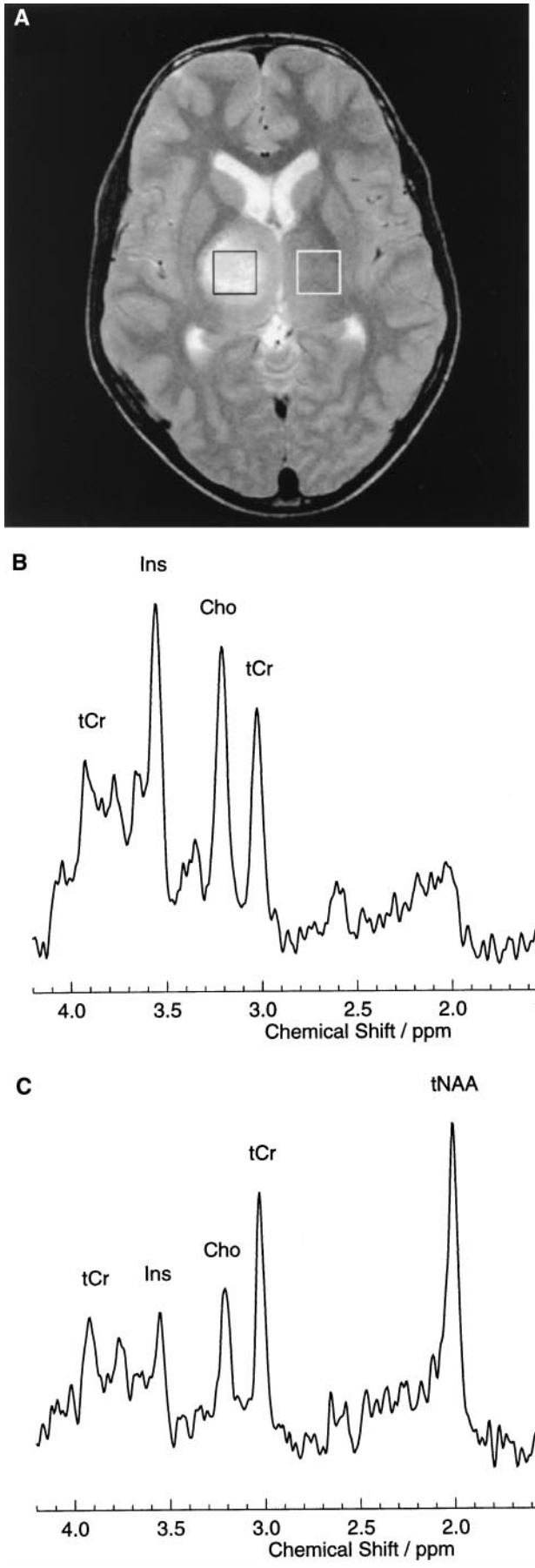

Figure 1. Anaplastic glioma III in a 13-year-old male (Patient 3). (A) T_2-weighted magnetic resonance image (fast-spin echo, TR = 2,625 ms, TE = 98 ms, flip angles 90 degrees/120 degrees) of a transverse section (thickness 4 mm) through the thalamus, indicating volumes-of-interest selected for proton magnetic resonance spectroscopy. (B,C) Corresponding proton magnetic resonance spectra (stimulated echo acquisition mode, TR = 6,000 ms, TE = 20 ms, TM = 10 ms, 64 accumulations, same scale) of the right hemispheric lesion and the contralateral side. Metabolite resonances refer to N-*acetylaspartate and* N-*acetylaspartylglutamate (tNAA), creatine and phosphocreatine (tCr), choline-containing compounds (Cho), and* myo-*inositol (Ins). The tumor was characterized by very low tNAA and strongly elevated Cho and Ins.*

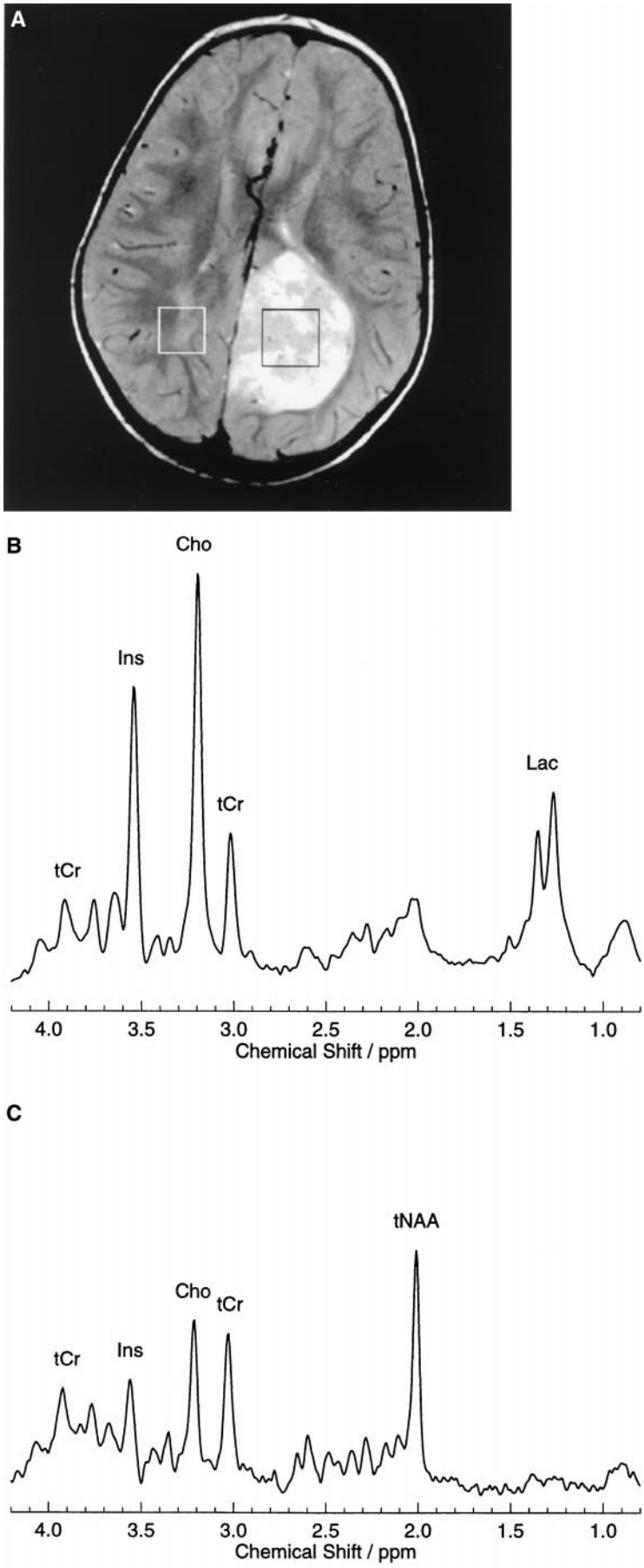

Figure 2. Primitive neuroectodermal tumor in a 1-year-old female (Patient 5). (A) T_2-weighted magnetic resonance image of a transverse section through the parietal cortex indicating volumes-of-interest selected for proton magnetic resonance spectroscopy. (B,C) Corresponding proton magnetic resonance spectra (same scale) of the left hemispheric lesion and the contralateral side (parameters as in Fig 1). The tumor was characterized by very low tNAA and strongly elevated Cho, Ins, and lactate (Lac). See Figure 1 for abbreviations.

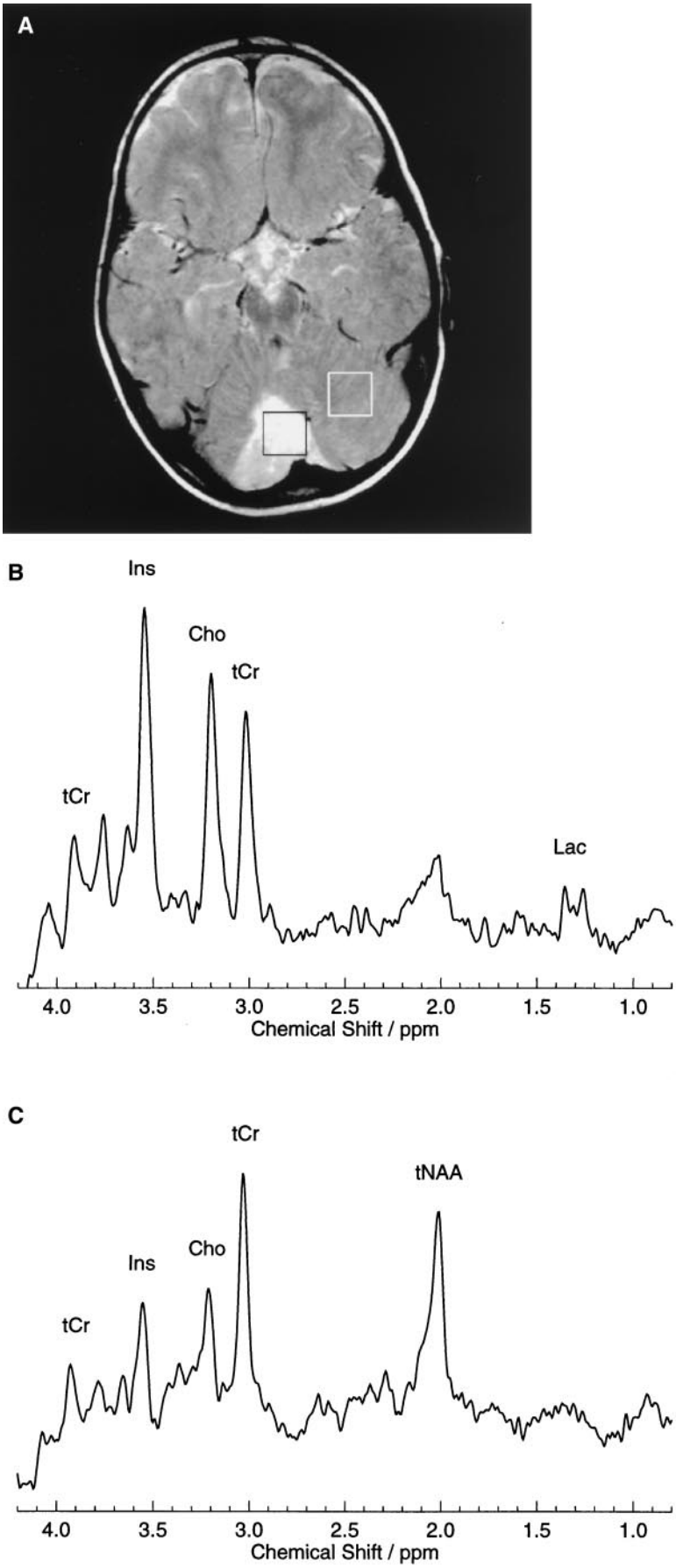

Figure 3. Pilocytic astrocytoma grade I in a 2-year-old female (Patient 9). (A) T_2-weighted magnetic resonance image of a transverse section through the cerebellum indicating volumes-of-interest selected for proton magnetic resonance spectroscopy. (B,C) Corresponding proton magnetic resonance spectra (same scale) of the right hemispheric lesion and the contralateral side (parameters as in Fig 1). The tumor was characterized by very low tNAA, strongly elevated Cho and Ins, and mildly elevated Lac. See Figures 1 and 2 for abbreviations.

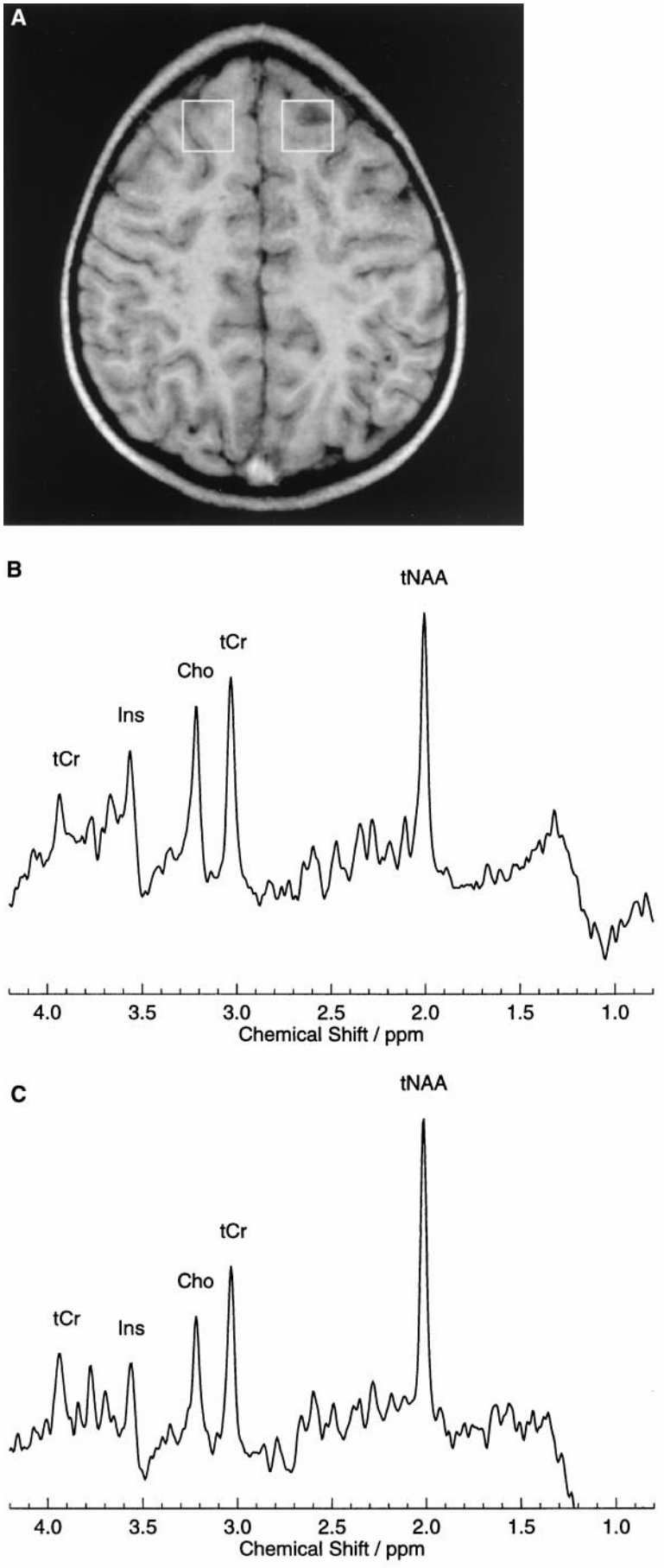

Figure 4. Gliosis in a 9-year-old male (Patient 14). (A) T_1-weighted magnetic resonance image (three-dimensional fast low-angle shot, TR = 15 ms, TE = 4 ms, flip angle 20 degrees) of a transverse section through the frontal cortex indicating volumes-of-interest selected for proton magnetic resonance spectroscopy. (B,C) Corresponding proton magnetic resonance spectra (same scale) of the left hemispheric lesion and the contralateral side (spectroscopy parameters as in Fig. 1). The gliosis was characterized by only mildly reduced tNAA and moderately elevated Cho and Ins. See Figure 1 for abbreviations.

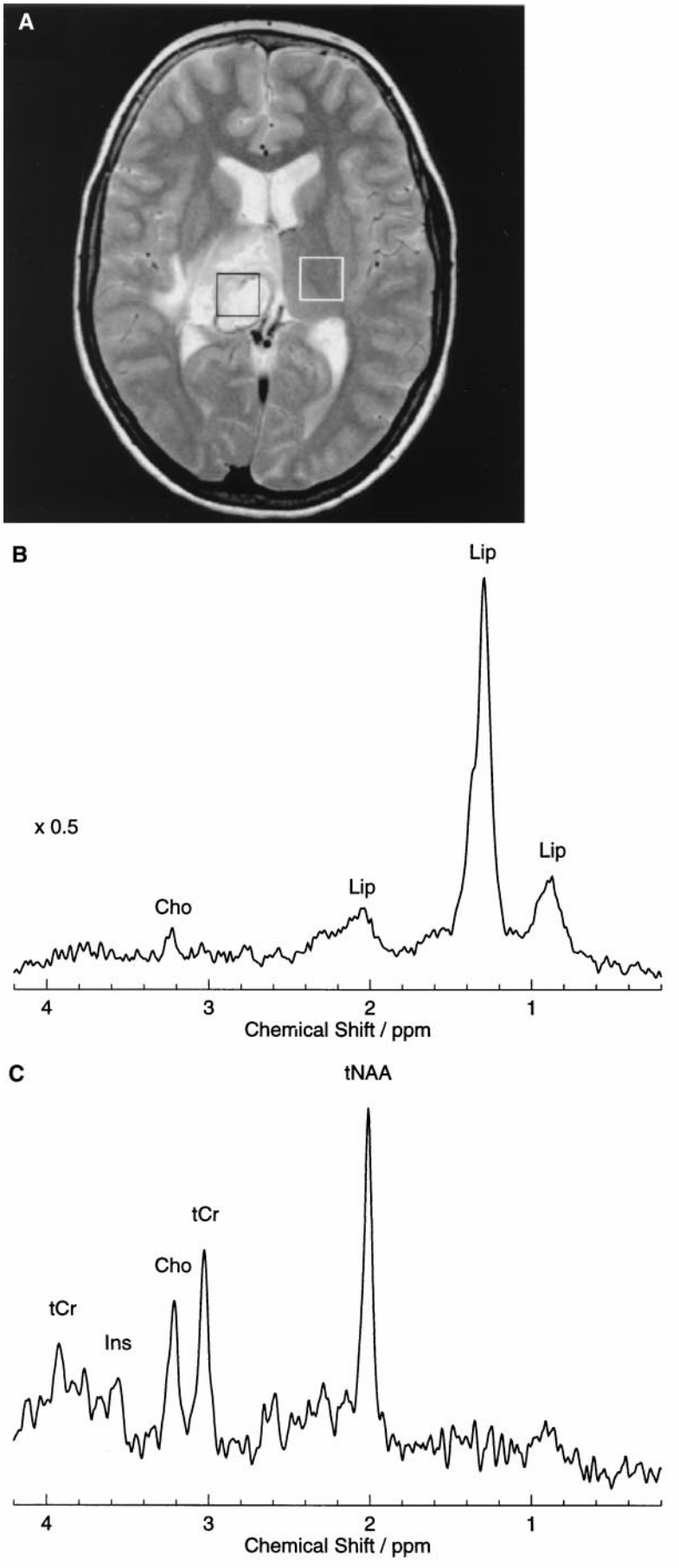

Figure 5. Abscess in an 11-year-old male (Patient 17). (A) T_2-weighted magnetic resonance image of a transverse section through the thalamus indicating volumes-of-interest selected for proton magnetic resonance spectroscopy. (B,C) Corresponding proton magnetic resonance spectra (scale differs by a factor of two) of the right hemispheric lesion and the contralateral side (parameters as in Fig. 1). The abscess was characterized by strong contributions from mobile lipids and a major loss of all metabolites, except for some residual choline-containing compounds (Cho).

MRI revealed a pronounced focal lesion in the right thalamus (Fig 5A). Even though the differential diagnosis was highly suspicious of infection, it included abscess and a brain tumor undergoing necrosis.

Although inflammation scintigraphy gave no clear result, the MR spectrum in Figure 5B demonstrates that the affected area was characterized by very strong contributions from mobile lipids and a generalized reduction of all metabolites that, except for Cho (1.1 mM vs 1.8 mM on the contralateral side and in the control subjects), were below detectability. The spectrum from the contralateral thalamic area in Figure 5C was normal.

The remarkable loss of brain tissue as evidenced by vanishing cellular metabolites together with the presence of large amounts of free lipids is significantly different from most viable brain tumors and from arachnoid cysts, which mainly contain cerebrospinal fluid and no lipids. On the other hand, the diagnostic hallmark of pronounced lipid contributions may result from several possibilities, including a central nervous system lymphoma [15], an abscess [16], or necrotic tissue [8,17]. Although the present findings were therefore classified as inconclusive, the neurosurgical intervention was guided by the assumption of an abscess. The histologic examination confirmed this hypothesis.

Proton MRS and Histopathologic Findings. The righthand part of Table 2 compares the in vivo metabolite findings with the histologic findings and evaluates the prognostic accuracy of proton MRS for tumor differential diagnosis. For this purpose, the spectroscopic results were retrospectively classified as correct, wrong, or of no value. The MRS assessment of unclear focal brain lesions in children was found to be correct in 14 (82%), wrong in one (6%), and of no added value in 2 (12%) of 17 patients.

Discussion

In agreement with previous studies of various brain disorders, the two most prominent pathologic processes in brain tissue that give rise to MRS-detectable alterations are a loss or damage of neuroaxonal tissue and the occurrence of glial proliferation [2,3]. Using tNAA and Ins as respective key markers, any reduction of neuroaxonal cells manifests itself as reduced tNAA (and glutamate) in proton MR spectra; however, growth of glial cells (mainly astrocytes) leads to increased Ins (and glutamine) or increased Cho (mainly oligodendrocytes), or both. As a constituent of both glial and neuronal cells, tCr may be reduced or enhanced, depending on the relative importance of the two processes. Strong variability is observed for Lac, which often reflects the anerobic metabolism of infiltrating macrophages and only rarely indicates mitochondrial dysfunction.

In this deliberately simplified context, primary brain tumors may be thought of as proliferated glial tissue free of neurons or axons. Their characteristic spectra exhibit very low if any tNAA and elevated Ins or Cho (or both). Using this pattern of metabolic alterations, we attempted to discriminate neoplasms from other focal brain lesions in our patient population. In 11 patients (Patients 1-11), tumors were correctly identified. These were mainly astrocytomas, which are closest to the combination of very low tNAA, high Ins or Cho, and variable Lac. In three patients (Patients 13-15), tumors were successfully excluded. Patients 14 and 15 had gliosis and proton MR spectra, which revealed the expected mild reduction of tNAA and only moderate increases of Ins and Cho. In Patient 13, multiple sclerosis led to a very low tNAA level but only a mild increase of Ins and no change of Cho and tCr.

Proton MRS failed in one case. A false-positive tumor diagnosis in Patient 12 was caused by a severe reactive gliosis mimicking a typical tumor spectrum with regard to low tNAA and high Ins. Two cases were inconclusive. Patient 16 presented with an astrocytoma causing only moderately elevated Ins and an atypical reduction of Cho, and Patient 17 presented with an abscess that led to a marked reduction of all metabolites but very strong contributions from mobile lipids.

In general, proton MRS helps to identify pathologic processes, such as a loss of neuroaxonal tissue and a proliferation of glial cells. However, instead of using selective ratios of T_1-weighted or T_2-weighted metabolite resonances, pertinent attempts should be based on multimetabolite patterns of absolute metabolite concentrations that should at least include tNAA, tCr, Cho, and Ins. Such patterns should be compared with data from individual control regions and from age-matched control subjects. Using this approach, the present work extends recent studies [7,8] in demonstrating a considerable clinical value of quantitative single-voxel proton MRS for preoperative characterization of focal brain lesions.

References

[1] **Packer** RJ. Childhood brain tumours: New directions in management. Eur J Pediatr Neurol 1997;5:133-8.

[2] **Frahm** J, Hanefeld F. Localized proton magnetic resonance spectroscopy of brain disorders in childhood. In: Bachelard HS, ed. Magnetic resonance spectroscopy and imaging in neurochemistry. New York: Plenum, 1997:329-402.

[3] **Danielsen** ER, Ross B. Magnetic resonance spectroscopy diagnosis of neurological disease. New York: Dekker, 1999.

[4] **Frahm** J, Bruhn H, Hänicke W, Merboldt KD, Mursch K, Markakis E. Localized proton NMR spectroscopy of brain tumors using short-echo time STEAM sequences. J Comput Assist Tomogr 1991;15: 915-22.

[5] **Falini** A, Calabrese G, Origgi D, et al. Proton magnetic resonance spectroscopy and intracranial tumours: Clinical perspectives. J Neurol 1996;243:706-14.

[6] **Bruhn** H, Frahm J, Gyngell ML, et al. Noninvasive differentiation of tumors with use of localized H-1 MR spectroscopy in vivo: Initial experience in patients with cerebral tumors. Radiology 1989; 172:541-8.

[7] **Girard** N, Wang ZJ, Erbetta A, et al. Prognostic value of proton MR spectroscopy of cerebral hemisphere tumors in children. Neuroradiology 1998;40:121-5.

[8] **Norfray** JF, Tomita T, Byrd SE, Ross BD, Berger PA, Miller RS. Clinical impact of MR spectroscopy when MR imaging is indeterminate for pediatric brain tumors. AJR Am J Roent 1999;173:119-25.

[9] **Frahm** J, Michaelis T, Merboldt KD, Bruhn H, Gyngell ML, Hänicke W. Improvements in localized 1H-NMR spectroscopy of human brain: Water suppression, short echo times, and 1 mL resolution. J Magn Reson 1990;90:464-73.

[10] **Pouwels** PJW, Frahm J. Regional metabolite concentrations in human brain as determined by quantitative localized proton MRS. Magn Reson Med 1998;39:53-60.

[11] **Provencher** SW. Estimation of metabolite concentrations from localized in vivo proton NMR spectra. Magn Reson Med 1993;30:672-9.

[12] **Birken** DL, Oldendorf WH. *N*-acetyl-L-aspartic acid: A litera-

ture review of a compound prominent in 1H NMR spectroscopic studies of brain. Neurosci Biobehav Rev 1989;13:23-31.

[13] **Brand** A, Richter-Landsberg C, Leibfritz D. Multinuclear NMR studies on the energy metabolism of glial and neuronal cells. Dev Neurosci 1993;15:289-98.

[14] **Pouwels** PJW, Brockmann K, Kruse B, et al. Regional age dependence of human brain metabolites from infancy to adulthood as detected by quantitative localized proton MRS. Pediatr Res 1999;46: 474-85.

[15] **Boyko** OB. Adult brain tumors. In: Stark DD, Bradley WG, eds. Magnetic resonance imaging, 3rd ed. St. Louis: Mosby, 1998: 1231-54.

[16] **Dev** R, Gupta RK, Poptani H, Roy R, Sharma S, Husain M. Role of in vivo proton magnetic resonance spectroscopy in the diagnosis and management of brain abscesses. Neurosurgery 1998;42:37-43.

[17] **Kuesel** AC, Sutherland GR, Halliday W, Smith ICP. ^{1}H-MRS of high grade astrocytomas: Mobile lipid accumulation in necrotic tissue. NMR Biomed 1994;7:149-55.